ACS OMEGA

http://pubs.acs.org/journal/acsodf

Article

Novel Reactive Distillation Process for Cyclohexyl Acetate Production: Design, Optimization, and Control

Yabo Hu, Le Wang, Jiawei Lu, Lianghui Ding, Guowen Zhang, Zhuxiu Zhang, Jihai Tang,* Mifen Cui, Xian Chen, and Xu Qiao*

Cite This: *ACS Omega* 2023, 8, 13192−13201

Read Online

ACCESS | Metrics & More | Article Recommendations | Supporting Information

ABSTRACT: A side-reactor column (SRC) configuration, comprising a vacuum column coupled with atmospheric side reactors, is proposed to overcome the thermodynamic restriction in the esterification of cyclohexene with acetic acid to produce cyclohexyl acetate. Meantime, this configuration can avoid the utilization of the high-pressure steam and provide enough zone for catalyst loading. In order to obtain the minimum total annual cost (TAC), the process is optimized by a mixed-integer nonlinear programming optimization method based on the improved bat algorithm. The results indicate that the optimized SRC configuration saves about 44.81% of the TAC compared to the reactive distillation process. Based on the optimized SRC process, dynamic control is carried out. The dual-point temperature and temperature-composition control structures are proposed to reject throughput and feed composition disturbances. The dynamic performances demonstrate that the temperature-composition control structure is better in maintaining product purity.

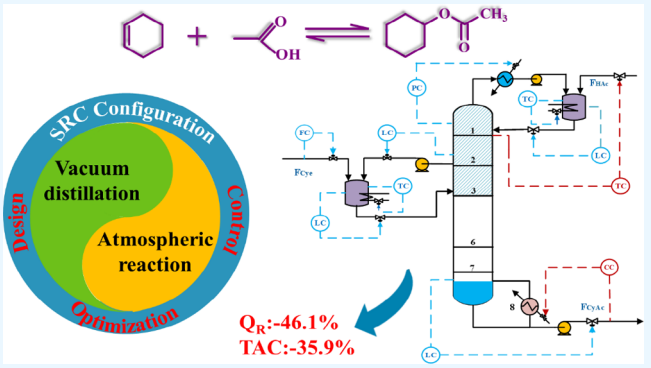

1. INTRODUCTION

Cyclohexanol is widely used as a vital chemical intermediate to synthesize adipic acid and ε-caprolactam.[1] At present, the industrial methods for the synthesis of cyclohexanol are oxidation of cyclohexane and direct hydration of cyclohexene,[2−4] as illustrated in Figure 1. The oxidation of cyclohexane poses a safety risk due to the formation of explosive mixtures in air.[5] With regard to the direct hydration of cyclohexene, despite high selectivity to cyclohexanol, the unsatisfactory conversion to about 12% results in the high energy consumption of separation of unreacted cyclohexane and the product.[6] To overcome the abovementioned limitations, a promising alternative process including cyclohexene esterification−hydrogenolysis with cyclohexyl acetate as an intermediate is proposed.[7,8] This route can also avoid the decomposition problem of formic acid in the reported indirect hydration with cyclohexyl formate as an intermediate.[9,10] Thus, the addition esterification of acetic acid with cyclohexene to produce cyclohexyl acetate is a key step.

However, the addition esterification of cyclohexene with carboxylic acid to produce cyclohexyl carboxylate is a reversible reaction. Reactive distillation (RD) is beneficial to reactions with limited equilibrium, which can effectively increase conversion[11−13] and energy saving[14−16] The RD process was developed for cyclohexyl formate, and the conversion of cyclohexene can achieve almost 100%. However, the temperature in the column must be controlled below 60 °C, which results in the mismatch between the operation conditions of reaction and separation.[10] There were only small differences in operational conditions for the RD process. Due to good stability, acetic acid was used to produce cyclohexyl acetate for cyclohexanol production, and the high cyclohexyl acetate yield of about 99.8% can be achieved in the RD process.[17] However, the column bottom temperature is high (about 173 °C), resulting in high-pressure steam used as utilities. The RD process cannot obtain an optimal match between the reaction and separation. Moreover, the catalyst loading is subject to the tray geometry.[18,19] In addition, some practical hardware limitations also exist, such as structured catalyst packing, catalyst replacement, and regeneration.

The side-reactor column (SRC) configuration is a competitive alternative to RD.[20,21] A non-RD column is connected by an external loop to the side reactors, which achieves the independent design between the reactor and the column. The SRC provides sufficient reaction zone for catalyst loading and is advantageous in catalyst replacement and maintenance. For propylene glycol monomethyl ether acetate production,[22] the

Received: January 23, 2023
Accepted: March 20, 2023
Published: March 30, 2023

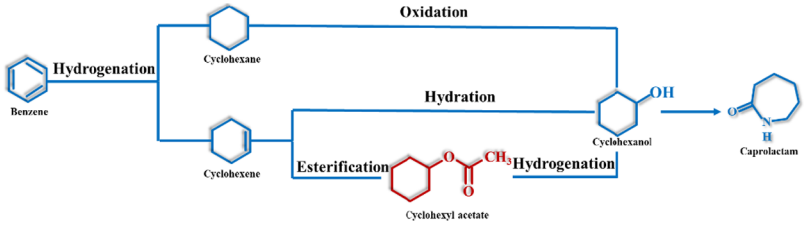

Figure 1. Reaction routes for production of caprolactam.

conflict of the RD configuration is the need of higher pressure for enhancing the reaction rate and the requirement for high-pressure steam in the reboiler. By contrast, the SRC configuration with a non-RD column can operate at 0.7 atm, and the reaction in the side reactor operates at 25 atm. The independent operation condition is provided with easy industrial scale-up. Moreover, the different conditions of reaction and separation in the SRC enable obvious increase in production capacity. Ding et al.[23] proposed an SRC process for the production of benzyl chloride with the pressures for reaction and separation being 101.3 and 10 kPa, respectively. The capacity of benzyl chloride increases by more than 60% compared to the RD configuration. The SRC process was also successfully applied in EtAc,[24] TAME,[25] and MeAc.[26]

A reliable control strategy is required to ensure the quality of the product in the continuous production process. So far, research studies on effective control for the SRC configuration are still scanty.[24,27−29] The multivariable control schemes for the SRC process show a good performance on the part of control precision. A robust, temperature-composition control strategy is designed to resist the feed flow rate and feed composition disturbances. Up to now, no literature has reported dynamic control of the process toward the production of cyclohexyl acetate. It is worth investigating an effective control scheme.

In this work, a novel SRC process integrating vacuum distillation and atmospheric reaction is established and investigated. Mixed-integer nonlinear programming (MINLP) optimization based on the improved bat algorithm[30] was used to realize global optimization for the SRC configuration. The RD process is also established, and the economics and energy consumption of the optimal RD and SRC configurations are compared. Moreover, the effective control structures for the SRC process are investigated. Feasible control structures are developed for the optimal SRC configuration in this work to reject the throughput and feed composition disturbances.

2. REACTION KINETICS AND THERMODYNAMICS

The esterification of cyclohexene (Cye) with acetic acid (HAc) to synthesize cyclohexyl acetate (CyAc) is expressed in eq 1. The reaction kinetics based on the Langmuir−Hinshelwood−Hougen−Watson (LHHW) model at the catalyst of sulfonic acid-type styrene cation exchange resin is shown in eq 2.[31] The heat of the reaction is 40 kJ/mol.

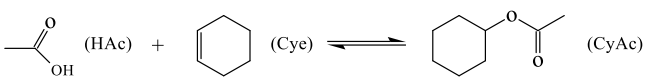

$$r_{CyAc} = \frac{5.33 \times 10^9 \exp\left(\frac{-93060}{RT}\right)\left(C_{HAc}C_{Cye} - \frac{C_{CyAc}}{\exp\left(\frac{4873}{T} - 13.813\right)}\right)}{(1 + 0.0437C_{HAc} + 0.2277C_{Cye} + 0.0992C_{CyAc})^2} \quad (2)$$

where r_{CyAc}, T, and c are the reaction rate, kmol/(kg min), the reaction temperature, K, and the mole concentration, kmol/m^3, respectively.

Figure 2 shows the residue curves map (RCM) diagram for the Cye-HAc-CyAc system in a normal atmosphere. To account

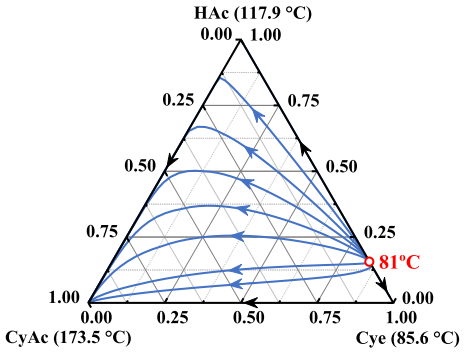

Figure 2. RCM diagram for the Cye-HAc-CyAc system at 1 atm.

for the nonideal phase behavior, the modified UNIFAC-DMD (Dortmund) model is used in this work to calculate the activity coefficient. As illustrated in Figure 2, there is a minimum boiling binary azeotrope (81 °C) between Cye and HAc at 0.84 molar fraction of Cye. Accordingly, the binary azeotrope and two reactants can be treated as light components, while the product CyAc is the heaviest component. The RCM in Figure 2 also indicates that it is possible to obtain a relatively high purity of CyAc in the bottom stream if most of the light reactants can be consumed in the top section, which is to be realized in the linked external side reactors.

3. PROCESS DESIGN AND OPTIMIZATION

3.1. Process Description of the SRC. Figure 3 depicts the SRC flowsheet for CyAc production. The boiling point of cyclohexyl acetate (173 °C) is high, and it can be obtained from the bottom. The boiling points of cyclohexene (81 °C) and acetic acid (118 °C) are low. They are concentrated in the top column, and the reactors are connected to the top column by external loops. The boiling point of cyclohexene is lower than that of acetic acid. Cyclohexene was fed in the lower reactor (R2), and acetic acid was fed in the upper reactor (R1). The overhead vapor from the column is condensed and introduced into the first side reactor (R1), and the reactor effluent is then fed back to the first stage for recycling. Similar to the above, the

https://doi.org/10.1021/acsomega.3c00469
ACS Omega 2023, 8, 13192−13201

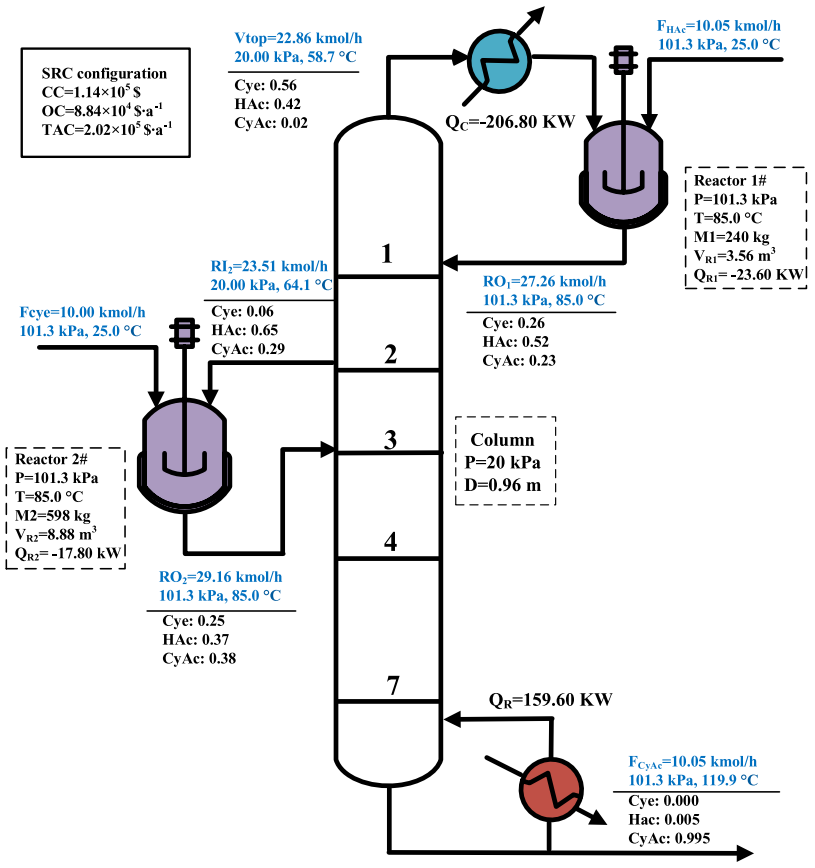

Figure 3. Optimized flowsheet of the SRC configuration for CyAc production.

total liquid from the liquid trap-out stage will be pumped into the second reactor (R2), and the reactor effluent is returned to the column on the stage below the trap-out stage from which it is withdrawn. The fresh feeds of HAc of 10.05 kmol/h and Cye of 10 kmol/h are set. Also, the purity of CyAc is set as 99.5 mol %.

The decision variables to be generated include the operating parameters, such as the operation conditions of the reactors and the distillation column, the catalyst loading within the reactors and the reboiler duty, etc., and the structural parameters, such as the number of side reactors, the locations of side-draw stages, etc. In order to simplify the optimization, the column pressure, reaction temperature, and pressure were determined through an empirical approach.[32−34] Under the appropriate basic configuration, the remaining structural and operating variables will be optimized with the detailed MINLP model. The objective function is to obtain the minimum total annual cost (TAC) for the process.

3.2. Decision of Operating Conditions. One of the advantages of the SRC is that the design variables of reaction and separation can be set independently.[35] In order to exploit the advantages of the SRC process for the CyAc system, the effects of the reaction temperature and column pressure are initially discussed. The continuous stirred tank reactor (CSTR) module is used to calculate the conversion of cyclohexene at a fixed residence time in different reaction temperatures. Figure 4 exhibits the effect of the reaction temperature on the conversion of cyclohexene under different catalyst weights. Note that the reactors are operated at atmospheric pressure, which is sufficiently high to keep the reactants in liquid phase at the discussed temperature range.

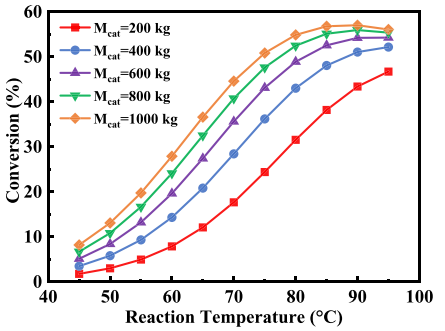

Figure 4. Effect of the reaction temperature on conversion under different catalyst weights M_{cat}.

As can be observed from Figure 4, for the suggested reaction temperature, when the reaction temperature begins to increase from 45 to 85 °C, there is an obvious rise in the conversion. A further increase in the reaction temperature leads to a relatively small change in the conversion. This phenomenon was also detected in the experiments reported in Chen et al.'s work.[31] The appropriate reaction temperature is eventually set to 85 °C. On the other hand, for the discussed catalyst loadings, as shown in Figure 4, an initial increase in the catalyst loading is favorable for the conversion. However, when the catalyst amount reaches 800 kg, further increasing the catalyst amount produces little effect on the reaction conversion. The catalyst amount is closely related to the reaction performance, which has significant impact on the reboiler duty required to achieve the desired purities of the product stream. The catalyst amount will be taken as a design

https://doi.org/10.1021/acsomega.3c00469
ACS Omega 2023, 8, 13192−13201

variable, and the range of the catalyst amount from 200 to 800 kg will be considered in the later optimization.

For the distillation column, the selection of the operating pressure can be determined under the overall consideration of the distillation performance and the selection of the available heat and cold utilities. The reduction in the column pressure brings about an obvious increase in the relative volatility of components. As illustrated in Figure 5, the relative volatility of

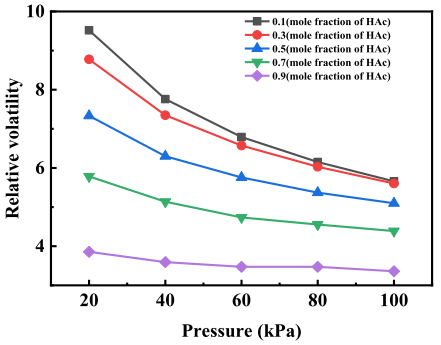

Figure 5. Effect of distillation pressure on relative volatility of HAc/CyAc.

HAc and CyAc at 20 kPa is about twice that at atmospheric pressure. A lower column pressure would significantly help to reinforce the separation ability to remove the produced CyAc from the reaction system so as to promote the forward reaction and improve the conversion. Meantime, it also helps to reduce the utilization of high-grade energy of stream. Figure 6 provides

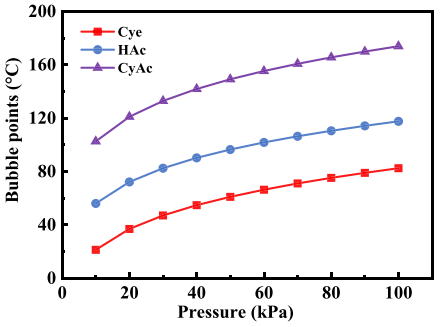

Figure 6. Boiling point of pure components under different pressures.

the effect of pressure on the boiling points of the pure components. As can be seen, when the pressure is set to 20 kPa, the column bottom temperature drops to about 120 °C, and the top temperature is about 45 °C, close to the minimum value through cooling water. Hence, the suitable operating pressure of the column is set to 20 kPa.

3.3. Optimization Procedure. Under the suggested reaction temperature and column pressure, the independent decision variables to be optimized in the SRC system include both a continuous variable (e.g., catalyst amount M_i) and discrete variables (e.g., the number of column stages N_{stage}, the number of side reactors NR, and the location of the trap-out stage FR_i). The optimization of the SRC aims to obtain the variables that minimize the TAC. The TAC, representing the trade-offs between capital and operating costs, is used as the objective function.

$$\text{TAC} = \frac{\text{Capital cost}}{\text{Payback period}} + \text{Operating cost} \tag{3}$$

A payback period of 3 years is used in the calculation of the TAC. The capital cost contained the costs of the column, reactors, and heat exchangers, which were calculated based on the correlations provided by Douglas[36] and were corrected by M&S.[37] The operating cost includes the cost of the catalyst, cooling water, and steam. The detailed TAC formulations and economic data are provided in Table S2. Hence, the optimization of the SRC can be formulated as an MINLP problem. Its mathematical expression is as follows:

Objective function

$$\min(\text{TAC}) = \min f(N\text{stage}, \text{NR}, \text{FRi}, Mi) \tag{4}$$

s.t.

$$f(w, N_{stage}, \text{NR}, \text{FR}_i, M_i) = 0 \tag{5}$$

$$lb_W \le y_W \tag{6}$$

$$lb \le \beta \le ub, x \in R^n \tag{7}$$

In this work, w is a vector of state variables determined by decision variables, which include the column diameter (D_c) and heat exchange area (A_c, A_R). Equation 5 represents the equality constraints, e.g., the process model equations; eq 6 represents the product purity constraints. lb and ub are the lower and upper bounds on the decision variables. y_w is the product purity.

In solving the MINLP problem, the complex interaction between the variables and the strong nonlinearity associated with the nonideal phase behavior and reaction kinetics lead to complexity in searching the global optimal values. In order to achieve nearly global optimal solutions, the improved bat algorithm, which has displayed excellent performance in the optimization of the complex nonlinear processes without requiring derivatives, is used as an optimizer for this MINLP model. Figure 7 exhibits the scheme of the optimization procedure. The execution of the improved bat algorithm and the calculation of the objective function are both implemented in MATLAB, while the Aspen Plus is used to solve the process models for each function evaluation. The communication

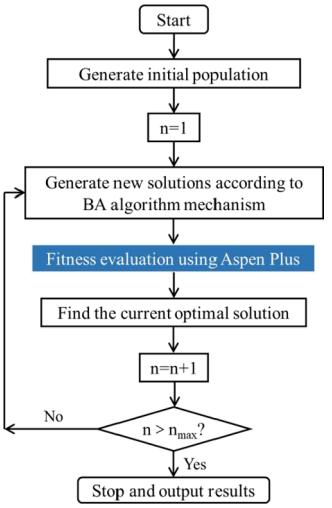

Figure 7. Scheme of the optimization procedure using MATLAB interfaced with Aspen Plus.

https://doi.org/10.1021/acsomega.3c00469
ACS Omega 2023, 8, 13192−13201

between MATLAB and Aspen Plus is realized through COM technology.[30,38,39]

Table 1 provides the types and bounds of the design variables in the optimization. All simulations and optimizations are carried out using a computer system running Windows 10, having an Intel Core i5 2.8 GHz processor and 8 GB RAM.

Table 1. Bounds and Types of Design Variables in the CyAc System

design variables	lower bound	upper bound	type
number of column stages N_{stage}	7	15	discrete
number of side reactors NR	1	3	discrete
location of the trap-out stage FR_i	2	$N_{stage} - 2$	discrete
catalyst amounts M_i/kg	200	800	continuous

4. RESULTS AND DISCUSSION

4.1. Optimization Results of the SRC. Considering the feature of the stochastic algorithm, three optimization runs (with different initial values of variables) have been executed to obtain the nearly global optimum values. The detailed stochastic optimization proceeding is presented in Figure 8. Figure 8 reveals that three optimization runs tend to be stable after generation 60, and the deviations of three TACs are small, implying that the optimization approach is robust and reliable.[30] The best result among them is taken as the optimum solution, as evidenced in Table 2. The results show that the optimal integrated configuration includes eight column stages and two side reactors, and the second side reactor is connected to the second stage. The amount of catalyst were 9.79 wt % and 9.81 wt % of the liquid holdup of R1 and R2, respectively. The side reactors are in a small amount of heat release, which not only avoids the use of steam but also ensures the safety of operation.

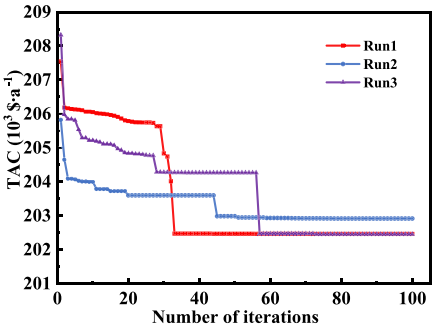

Figure 8. Optimization process with three different runs.

Figure 9 depicts the liquid composition and temperature profiles in the column of optimal design. As depicted in Figure 9a, HAc is abundant in the second stage where the concentration of CyAc is insufficient. It is beneficial for esterification to withdraw liquid from this position and pump it into the side reactor, suggesting rationality of the optimization results. Stages 3−8 aim to remove the reactants Cye and HAc, thereby achieving the purification of CyAc. No obvious platform appears on the composition and temperature profiles, indicating that there is no waste of stages and the results are reasonable and reliable.

4.2. Comparison of RD and SRC Processes. The obtained optimized SRC process is also compared with the RD process, and the results of the comparison are listed in Table 3. A detailed description of the RD process and the corresponding optimization procedure is provided in the Supporting Information (Reactive Distillation Configuration and Optimization). In the SRC process, the reaction did not occur in the column, and there was no need to set the reactive section. Therefore, the number of total stages in the column is greatly reduced from 24 to 8 with an obvious reduction in the reboiler duty of 46.1%. This displays that the design variables for reaction and separation can be set independently in the SRC process. Moreover, owing to the facile reduction of the column bottom temperature to 120 °C, the SRC can use medium-pressure steam (about 160 °C) instead of high-pressure steam (about 210 °C) to heat the reboiler, thus reducing the operating cost by 52.8%. However, the increased column diameter due to vacuum operation and the extra side reactors lead to an increase in capital cost. Overall, the TAC of the SRC configuration is saved up to 44.81% in comparison with the atmospheric RD process. Furthermore, if we compare the SRC with vacuum RD, it is indicated that the SRC has a more significant economic advantage owing to the solution of temperature mismatch between reaction and separation.

Table 2. Optimization Results of the SRC Configuration for the CyAc System

design variables	results
column stage number N_{stage}	8
column diameter (m)	0.96
column pressure (kPa)	20
condenser duty (kW)	206.79
reboiler duty (kW)	159.57
side reactor number NR	2
side-draw locations FR_i	0/2
reaction pressure (kPa)	101.3
reaction temperature (°C)	85
reactor duty (kW)	−23.60/−17.84
catalyst amount in side reactors (kg)	240/598
side reactor volume (m^3)	3.56/8.88
product CyAc purity (% mol/mol)	99.5%
annual operation cost ($ a^{-1})	8.84×10^4
annual average capital cost ($ a^{-1})	1.14×10^5
TAC ($ a^{-1})	2.02×10^5

5. PROCESS CONTROL

5.1. Controlling Variable Analysis. The control structures of the optimal SRC configuration are also investigated in this section. The objective of control strategies is to maintain the product purity of 99.5 mol % under the throughput and feed composition disturbances. It is necessary to determine the equipment sizes (side reactors and column bases) before turning the steady-state simulation in Aspen Plus into a dynamic simulation in Aspen Dynamics. The sump of the column is usually sized to provide 5 min of liquid holdup when 50% of the vessel is filled. The weir height is set to 0.025 m, while the stage pressure drop is specified as 0.0068 atm.[32,40] The sizes of the side reactors have been determined in the steady-state simulation, as recorded in Table 2, and the liquid holdup accounts for 75% full in the dynamic initialization. Moreover, it is assumed that the liquid on the side-draw stage is fully withdrawn into the side reactor in a steady-state design, while the side stream flow rate is fixed at 23.51 kmol/h (optimal design result) in a dynamic simulation.

https://doi.org/10.1021/acsomega.3c00469
ACS Omega 2023, 8, 13192−13201

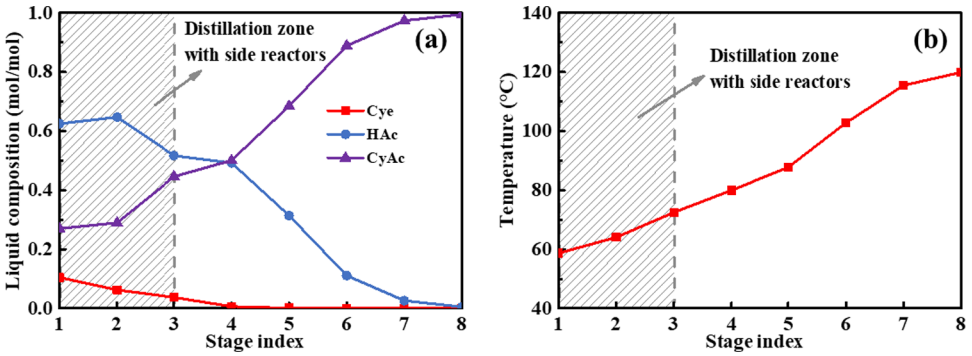

Figure 9. (a) Liquid composition and (b) temperature profiles in the distillation column.

Table 3. Comparison of Key Economic Indicators for the RD and SRC Designs

design variables	RD	SRC	comparison (%)
column stage number N_{stage}	24	8	
column diameter (m)	0.88	0.96	9.10
column pressure (kPa)	101.33	20	
condenser duty (kW)	337.21	206.79	−38.70
reboiler duty (kW)	295.80	159.57	−46.10
reactor heating duty (kW)	0	−23.60/−17.84	
reboiler temperature (°C)	172.10	119.90	
reaction temperature (°C)	80∼95	85	
total catalyst amount (kg)	383	838	118.80
annual operation cost ($ a^{-1})	**1.88×10^5**	**8.84×10^4**	**−52.80**
catalyst cost ($ a^{-1})	5.89×10^3	1.29×10^4	119.20
steam cost ($ a^{-1})	1.67×10^5	6.47×10^4	−61.20
cooling water cost ($ a^{-1})	1.47×10^4	1.08×10^4	−26.70
annual average capital cost ($ a^{-1})	**1.78×10^5**	**1.14×10^5**	**35.96**
side reactor cost ($)	0	4.02×10^4	
column cost ($)	2.72×10^5	1.18×10^5	−56.62
heat exchanger costs ($)	2.60×10^5	1.84×10^5	−29.23
TAC ($ a^{-1})	**3.66×10^5**	**2.02×10^5**	**44.81**

For the SRC configuration of CyAc production, there are five inventory variables, including the column pressure and four liquid level control loops (the sump level, side-draw stage liquid level, and two side reactor liquid levels). The column pressure is controlled by manipulating the heat removal rate in the condenser of the column. The sump and side-draw stage liquid level are controlled by the bottom flow rate and side stream flow rate, respectively. Each side reactor liquid level is controlled by manipulating their corresponding outlet flow rate, and the reactor temperature is maintained by manipulating the cooling water. The gains and integral times of the pressure and level controllers are taken from the literature as reported by Luyben.[40] The gains and integral times are expressed in eqs 8 and 9.

$$K_c = \frac{K_u}{3.2} \tag{8}$$

$$\tau_I = 2P_u \tag{9}$$

After closing these control loops, there are three independent manipulated variables: Cye feed flow rate (F_{Cye}), HAc feed flow rate (F_{HAc}), and reboiler heat duty (Q_R). Previous work[24,41] has proven that a two-temperature control structure, where the two fresh feeds are manipulated to control two stage temperatures, cannot provide effective control for the SRC configuration. Hence, in this work, the variables of F_{HAc} and Q_R are adopted in the design of the control structure with the feed flow rate of Cye directly controlled by a throughput valve. On this basis, two control structures, namely, dual-point temperature and temperature-composition control structures, are proposed, and the dynamic performances under throughput and feed composition disturbances are then investigated in detail.

5.2. Process Control Structure. *5.2.1. Dual-Point Temperature Control Structure.* Figure 10a exhibits the dual-point temperature control structure (CS1) in the optimal SRC process. One of the significant issues in designing the temperature control structure is selecting the column stage where the temperature should be controlled. In order to determine the position of the sensitive stage, the open-loop steady-state sensitivities (gains) of the stage temperature are checked by slightly decreasing (−0.1%) the manipulated variables F_{HAc} and Q_R. The results are illustrated in Figure 11a. Then, singular value decomposition (SVD) is also performed on the relative gain matrix to obtain a matrix U, as displayed in Figure 11b. The results of SVD are similar to that of sensitivity analysis, and both indicate that the properly controlled stages are the 1st and the 6th with clear peaks. According to the closely paired rule, the manipulated variables F_{HAc} and Q_R are, respectively, used to control the temperatures in the 1st and the 6th stages. It is necessary for the rapid recovery of dynamic performance to set the controller settings. Table 4 lists the controller settings for all loops in CS1.

Figure 12 demonstrates the dynamic responses of the CS1 for the SRC process after introducing ±10% throughput and −5% feed composition disturbances. These disturbances can evaluate the robustness of the control structure. It can be observed that the HAc feed flow rate and reboiler heat duty are automatically regulated to meet the reaction stoichiometric ratio with the introduction of disturbances, and the system stabilizes after 5−10 h. However, the specified product purity of 0.995 cannot be

https://doi.org/10.1021/acsomega.3c00469
ACS Omega 2023, 8, 13192−13201

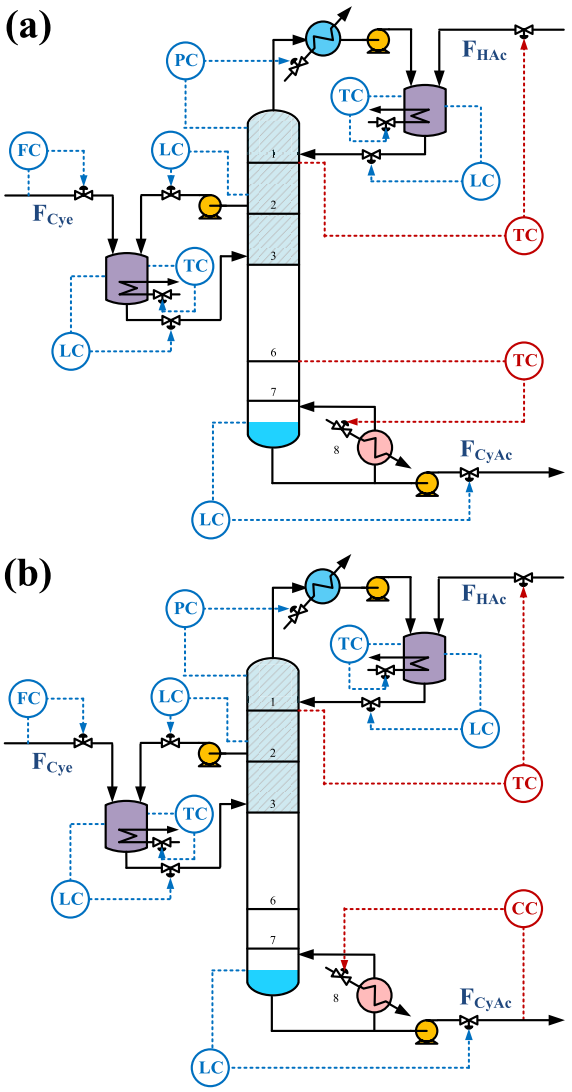

Figure 10. (a) Dual-point temperature control structure and (b) temperature-composition control structure.

easily achieved under the disturbances. When the product purity specification is not strict, the dual-point temperature control structure is acceptable for the stable operation of the SRC process. Here, the control structure with composition controllers is further considered in the next section to improve the dynamic performances.

Table 4. Controller Settings for Dual-Point and Temperature-Composition Control Structures

controller		controlled variable	manipulated variable	PID settings CS1	CS2
LC	P	reactor 1 level	valve position in reactor 1 outlet	$K_c = 10$, $\tau_I = 60$	
		reactor 2 level	valve position in reactor 2 outlet	$K_c = 10$, $\tau_I = 60$	
		stage 2 level	stream flow rate in stage 2	$K_c = 2$	
		sump level	stream flow rate in the reboiler	$K_c = 2$	
PC	PI	column pressure	condenser heat removal	$K_c = 20$, $\tau_I = 12$	
FC	PI	cye feed flow rate	valve position	$K_c = 0.50$, $\tau_I = 0.30$	
TC	PI	reactor 1 temperature	coolant flow rate in reactor 1	$K_c = 52.70$, $\tau_I = 11.80$	
		reactor 2 temperature	coolant flow rate in reactor 2	$K_c = 42.30$, $\tau_I = 3.90$	
		1st tray temperature	HAc feed flow rate	$K_c = 5$	
		6th tray temperature	reboiler duty	$K_c = 92.4$, $\tau_I = 5.30$	
CC	PI	CyAc product purity	reboiler duty		$K_c = 15.3$, $\tau_I = 6.50$

5.2.2. Temperature-Composition Control Structure. Figure 10b exhibits the temperature-composition control structure (CS2). Compared with CS1, CS2 removes the control of the temperature in the 6th stage and instead directly uses the reboiler heat duty (Q_R) to control the column bottom product purity. The manipulated variable F_{HAc} is still used to control the temperature in the 1st stage. Table 4 lists the controller settings for all loops in CS2. Figure 13 provides the dynamic performances of the CS2 under throughput and feed composition disturbances. The dynamic response of F_{HAc} and Q_R of CS2 is similar to that of CS1, both of which satisfy the stoichiometric ratio. The product purity is maintained at the specified value of 0.995, which is significantly improved compared to CS1. However, the response time to reach the steady state increases, especially when the HAc composition is disturbed. It takes about 15 h to get back to stability. In addition, since online component analyzers are usually expensive and require high maintenance costs, it is more practical to use temperature measurements in process control. If the product purity allows slight fluctuations, the dual-point temperature control structure is still the prior choice.

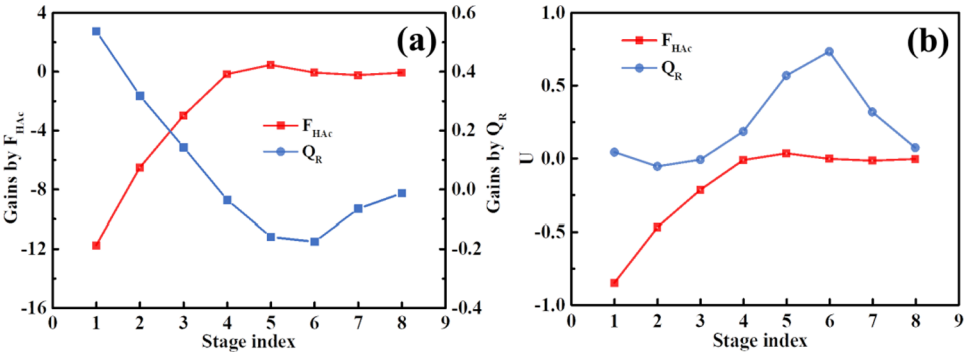

Figure 11. (a) Steady-state sensitivities and (b) SVD analysis.

https://doi.org/10.1021/acsomega.3c00469
ACS Omega 2023, 8, 13192−13201

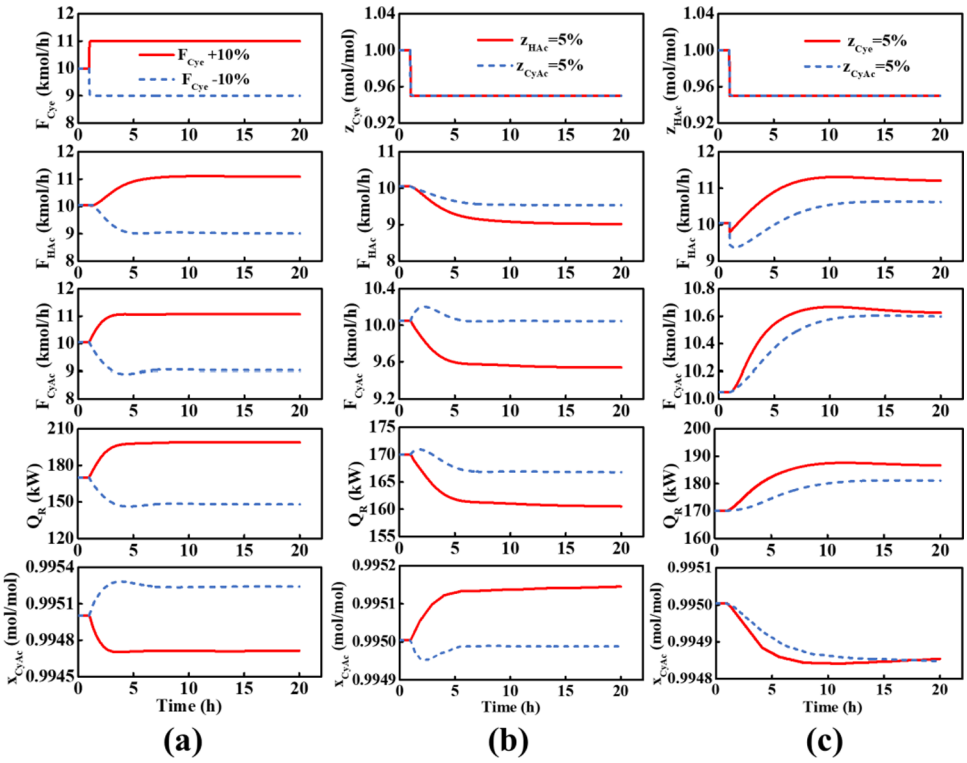

Figure 12. Dynamic responses of dual-point temperature control. (a) ±10% Cye feed flow disturbance; (b) −5% Cye feed composition disturbance; and (c) −5% HAc feed composition disturbance.

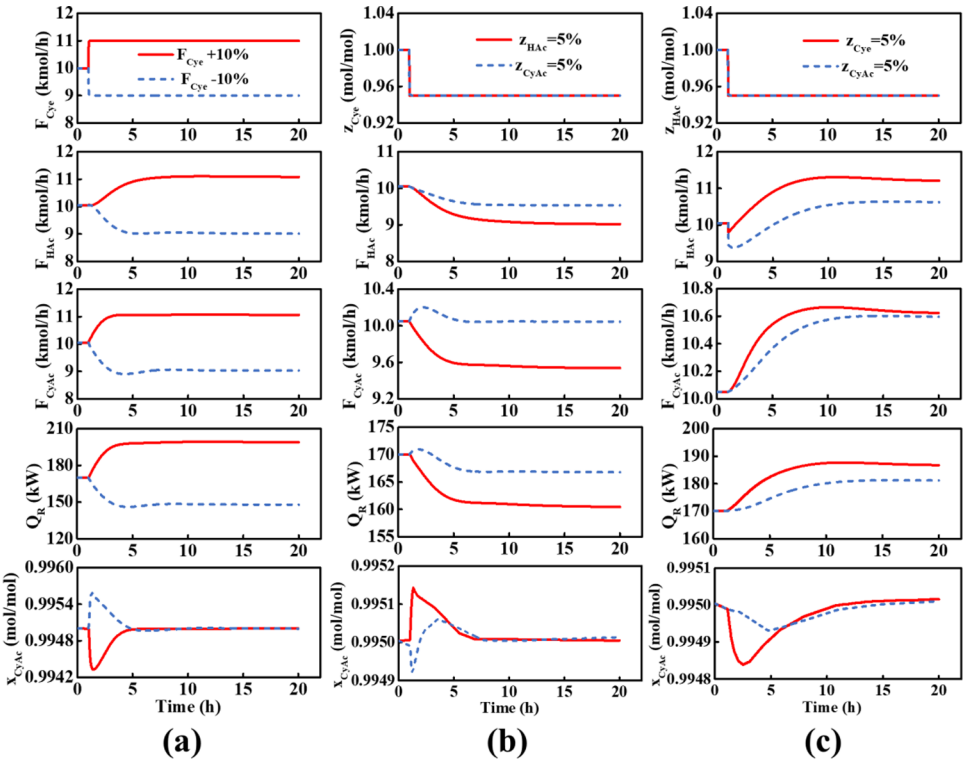

Figure 13. Dynamic responses of temperature-composition control. (a) ±10% Cye feed flow disturbance; (b) −5% Cye feed composition disturbance; and (c) −5% HAc feed composition disturbance.

6. CONCLUSIONS

In order to solve the mismatch between the distillation temperature and the reaction temperature in this system, an SRC configuration, which integrates vacuum distillation with atmospheric reaction, was developed for CyAc production. With the TAC as the optimization target, the optimized operating parameters and structural parameters were acquired using the improved bat algorithm to realize the perfect match of the

https://doi.org/10.1021/acsomega.3c00469
ACS Omega 2023, 8, 13192−13201

reaction and separation capacity. The results indicate that the optimized SRC configuration saves about 44.81% of the TAC and 52.81% of the operation cost compared to the RD process.

In addition, two control strategies, including the dual-point temperature and temperature-composition control structures, were proposed for the SRC process to reject the throughput and feed composition disturbances. The dynamic performances demonstrate that both control structures achieve effective control under those disturbances, but the temperature-composition control structure maintains the specified product purity more strictly than the dual-point temperature control structure. Based on the study of the integrated configuration and dynamics of the SRC, a reference for industrial design is provided.

■ ASSOCIATED CONTENT

Supporting Information

The Supporting Information is available free of charge at https://pubs.acs.org/doi/10.1021/acsomega.3c00469.

Validation of the thermodynamic model; detailed TAC formulations; RD configuration and optimization; optimized flowsheet of the RD configuration for CyAc production; and detailed optimization results and discussion for the RD process (PDF)

■ AUTHOR INFORMATION

Corresponding Authors

Jihai Tang − *State Key Laboratory of Materials-Oriented Chemical Engineering, College of Chemical Engineering, Nanjing Tech University, Nanjing 211816, PR China;* orcid.org/0000-0002-8166-9958; Phone: +86 025-83172298; Email: jhtang@njtech.edu.cn; Fax: +86 025-83587168

Xu Qiao − *State Key Laboratory of Materials-Oriented Chemical Engineering, College of Chemical Engineering, Nanjing Tech University, Nanjing 211816, PR China*; Phone: +86 025-83172298; Email: qct@njtech.edu.cn; Fax: +86 025-83587168

Authors

Yabo Hu − *State Key Laboratory of Materials-Oriented Chemical Engineering, College of Chemical Engineering, Nanjing Tech University, Nanjing 211816, PR China*

Le Wang − *State Key Laboratory of Materials-Oriented Chemical Engineering, College of Chemical Engineering, Nanjing Tech University, Nanjing 211816, PR China*

Jiawei Lu − *State Key Laboratory of Materials-Oriented Chemical Engineering, College of Chemical Engineering, Nanjing Tech University, Nanjing 211816, PR China*

Lianghui Ding − *School of Environmental Engineering, Nanjing Institute of Technology, Nanjing, Jiangsu 211167, China*

Guowen Zhang − *State Key Laboratory of Materials-Oriented Chemical Engineering, College of Chemical Engineering, Nanjing Tech University, Nanjing 211816, PR China*

Zhuxiu Zhang − *State Key Laboratory of Materials-Oriented Chemical Engineering, College of Chemical Engineering, Nanjing Tech University, Nanjing 211816, PR China*

Mifen Cui − *State Key Laboratory of Materials-Oriented Chemical Engineering, College of Chemical Engineering, Nanjing Tech University, Nanjing 211816, PR China*

Xian Chen − *State Key Laboratory of Materials-Oriented Chemical Engineering, College of Chemical Engineering, Nanjing Tech University, Nanjing 211816, PR China;* orcid.org/0000-0003-3046-0123

Complete contact information is available at: https://pubs.acs.org/10.1021/acsomega.3c00469

Notes

The authors declare no competing financial interest.

■ ACKNOWLEDGMENTS

The authors acknowledge financial support from the National Key R&D Program of China (2017YFB0307304), the Natural Science Foundation of China (21276126, 21676141, 61673205), the Key R&D Program of Jiangsu Province (BE2021710), the Qinglan Project of Jiangsu Province, and a project funded by the Priority Academic Program Development of Jiangsu Higher Education Institutions (PAPD).

■ NOMENCLATURE

r_i = reaction rate, kmol/(kg min)
T = temperature, K
c = mole concentration, kmol/m^3
V_{top} = vapor rate of the column top to the side reactor, kmol/h
F_{HAc} = feed rate of acetic acid to the side reactor, kmol/h.
F_{Cye} = feed rate of cyclohexene to the side reactor, kmol/h
RO_i = outlet flow rate from the side reactor, kmol/h
RI_i = inlet flow rate to the side reactor, kmol/h
M_i = catalyst amount, kg
VR_i = side reactor volume, m^3
QR_i = reactor duty, kW
N_{stage} = column stage number
NR = side reactor
FR_i = side-draw locations

Abbreviations

Cye = cyclohexene
HAc = acetic acid
CyAc = cyclohexyl acetate
TAC = total annual cost
MINLP = mixed-integer nonlinear programming
RD = reactive distillation
SRC = side reactor column
x = molar fraction
β = vector of decision variables
lb, ub = lower and upper bounds on the decision variables β
w = vector of state variables determined by decision variables

■ REFERENCES

(1) Zhu, Y. F.; Gao, L.; Wen, L. Y.; Zong, B. N.; Wang, H.; Qiao, M. H. Cyclohexene esterification-hydrogenation for efficient production of cyclohexanol. *Green Chem.* **2021**, *23*, 1185−1192.

(2) Wang, X. Y.; Feng, X. Y.; Liu, J. C.; Huang, Z. L.; Zong, S.; Liu, L. L.; Liu, J. R.; Fang, Y. X. Photo-thermo catalytic selective oxidation of cyclohexane by In-situ prepared nonstoichiometric Molybdenum oxide and Silver-palladium alloy composite. *J. Colloid Interf. Sci.* **2022**, *607*, 954−966.

(3) Feng, Y.; Jia, C. Q.; Zhao, H.; Wang, K.; Wang, X. T. Phase-dependent photocatalytic selective oxidation of cyclohexane over copper vanadates. *New J. Chem.* **2022**, *46*, 4082−4089.

(4) Wang, Q. L.; Zhang, F. Y.; Huang, R.; Wang, X. D.; Yang, C.; Wang, H. X.; Qiu, T. Multiphase flow and multicomponent reactive transport study in the catalyst layer of structured catalytic packings for the direct hydration of cyclohexene. *Chem. Eng. Process.* **2020**, *158*, No. 108199.

(5) Fang, X.; Yin, Z.; Wang, H.; Li, J. X.; Liang, X. P.; Kang, J. L.; He, B. Q. Controllable oxidation of cyclohexane to cyclohexanol and

cyclohexanone by a nano-MnOx/Ti electrocatalytic membrane reactor. *J. Catal.* **2015**, *329*, 187−194.
(6) Meng, F. J.; Wang, Y. Q.; Wang, S. G.; Wang, S. H. Hydration of cyclohexene over zeolite ZSM-5: improved catalyst performance by alkali treatment. *Reac. Kinet. Mech. Cat.* **2016**, *119*, 671−683.
(7) Song, T. Y.; Chen, W.; Qi, Y. Y.; Wu, P.; Zhu, Z. R.; Li, X. H. Efficient Synthesis of Cyclohexanol and Ethanol via the Hydrogenation of Acetic Acid-Derived Cyclohexyl Acetate with the $CuxAl_1Mn_{2-x}$ Catalysts. *ChemCatChem* **2021**, *13*, 3099−3111.
(8) Guang, B. X.; Wu, Y. F.; Liu, W. H.; Wang, J. H.; Xiao, Y. H.; Liu, Y. Kinetics Study of the Esterification Reaction of Cyclohexene to Cyclohexyl Acetate Catalyzed by Novel Bronsted-Lewis Acids Bifunctionalized Heteropolyacid Based Ionic Liquids Hybrid Solid Acid Catalysts. *Catal. Lett.* **2022**, *152*, 75−86.
(9) Pappu, V. K. S.. *Process Intensification in the Synthesis of Organic Esters: Kinetics, Simulations and Pilot Plant Experiments*; Michigan State University, 2012, 1−213.
(10) Katariya, A.; Freund, H.; Sundmacher, K. Two-Step Reactive Distillation Process for Cyclohexanol Production from Cyclohexene. *Ind. Eng. Chem. Res.* **2009**, *48*, 9534−9545.
(11) Kiss, A. A.; Jobson, M.; Gao, X. Reactive Distillation: Stepping Up to the Next Level of Process Intensification. *Ind. Eng. Chem. Res.* **2019**, *58*, 5909−5918.
(12) Segovia-Hernandez, J. G.; Hernandez, S.; Petriciolet, A. B. Reactive distillation: A review of optimal design using deterministic and stochastic techniques. *Chem. Eng. Process.* **2015**, *97*, 134−143.
(13) Zhang, Y. Z.; He, N.; Masuku, C. M.; Biegler, L. T. A multi-objective reactive distillation optimization model for Fischer-Tropsch synthesis. *Comput. Chem. Eng.* **2020**, *135*, No. 106754.
(14) Chen, Z. H.; Zhang, Z. S.; Zhou, J. B.; Chen, H.; Li, C. M.; Li, X. G.; Li, H.; Gao, X. Efficient Synthesis of Isobutylene Dimerization by Catalytic Distillation with Advanced Heat-Integrated Technology. *Ind. Eng. Chem. Res.* **2021**, *60*, 6121−6136.
(15) Gao, X.; Wang, Y. W.; Wang, R.; Dai, C. N.; Chen, B. H.; Zhu, J. Q.; Li, X. G.; Li, H.; Lei, Z. G. Application of Dimethyl Carbonate Assisted Chemical Looping Technology in the Separation of the Ethylene Glycol and 1,2-Butanediol Mixture and Coproduction of 1,2-Butene Carbonate. *Ind. Eng. Chem. Res.* **2021**, *60*, 2249−2264.
(16) Wang, R.; Li, X. G.; Na, J.; Wu, Y.; Zhao, R. N.; Yan, Y. T.; Li, H.; Gao, X. Reversible reaction-assisted intensification process for separating ethanediol and 1, 2-butanediol: Competitive kinetics study and conceptual design. *Sep. Purif. Technol.* **2020**, *237*, No. 116323.
(17) Deng, T.; Zhao, G. F.; Liu, Y.; Lu, Y. Catalytic distillation for one-step cyclohexyl acetate production and cyclohexene-cyclohexane separation via esterification of cyclohexene with acetic acid over microfibrous-structured Nafion-SiO_2/SS-fiber packings. *Chem. Eng. Process.* **2018**, *131*, 215−226.
(18) Hussain, A.; Lee, M. Optimal design of an intensified column with side-reactor configuration for the methoxy-methylheptane process. *Chem. Eng. Res. Des.* **2018**, *136*, 11−24.
(19) Ye, J. C.; Li, J.; Sha, Y.; Lin, H. D.; Zhou, D. W. Evaluation of Reactive Distillation and Side Reactor Configuration for Direct Hydration of Cyclohexene to Cyclohexanol. *Ind. Eng. Chem. Res.* **2014**, *53*, 1461−1469.
(20) Jakobsson, K.; Pyhalahti, A.; Pakkanen, S.; Keskinen, K.; Aittamaa, J. Modelling of a side reactor configuration combining reaction and distillation. *Chem. Eng. Sci.* **2002**, *57*, 1521−1524.
(21) Ding, L. H.; Tang, J. H.; Qiao, X.; Liu, C. R.; Xue, Y. B.; Wu, G. D. Design and analysis of an intensified column with side reactor configuration for ethylene glycol production from ethylene oxide. *Chem. Eng. Process.* **2020**, *147*, No. 107744.
(22) Hussain, A.; Chaniago, Y. D.; Riaz, A.; Lee, M. Process Design Alternatives for Producing Ultra-high-purity Electronic-Grade Propylene Glycol Monomethyl Ether Acetate. *Ind. Eng. Chem. Res.* **2019**, *58*, 2246−2257.
(23) Ding, L. H.; Tang, J. H.; Cui, M. F.; Chen, X.; Bo, C. M.; Qiao, X. Analysis and comparison of RD and SRC involving consecutive reaction of chlorination of toluene. *CIESC J.* **2013**, *64*, 3277−3284.
(24) Tsai, R. C.; Cheng, J. K.; Huang, H. P.; Yu, C. C.; Shen, Y. S.; Chen, Y. T. Design and Control of the Side Reactor Configuration for Production of Ethyl Acetate. *Ind. Eng. Chem. Res.* **2008**, *47*, 9472−9484.
(25) Nava, J. A. O.; Baur, R.; Krishna, R. Combining distillation and heterogeneous catalytic reactors. *Chem. Eng. Res. Des.* **2004**, *82*, 160−166.
(26) Baur, R.; Krishna, R. Distillation column with reactive pump arounds: an alternative to reactive distillation. *Chem. Eng. Process.* **2004**, *43*, 435−445.
(27) Kaymak, D. B.; Luyben, W. L. Dynamic Control of a Column/Side-Reactor Process. *Ind. Eng. Chem. Res.* **2008**, *47*, 8704−8712.
(28) Bo, C.; Huang, Q.; Tang, J.; Zhang, G.; Qiao, X. Multi-variable dynamic control of distillation column with side reactors for methyl acetate production. *CIESC J.* **2016**, *67*, 919−924.
(29) Zhang, G. W.; Wang, L.; Tang, J. H.; Jin, H.; Zhang, Z. X.; Fei, Z. Y.; Liu, Q.; Chen, X.; Cui, M. F.; Qiao, X. Design and Control for the Dimethyl Adipate Process with a Side-Reactor Column Configuration. *Chem. Eng. Technol.* **2021**, *44*, 1716−1725.
(30) Lu, J. W.; Kong, Q.; Zhang, Z. X.; Tang, J. H.; Cui, M. F.; Chen, X.; Liu, Q.; Fei, Z. Y.; Qiao, X. MINLP Optimization of Side-Reactor Column Configuration Based upon Improved Bat Algorithm. *Ind. Eng. Chem. Res.* **2020**, *59*, 5945−5955.
(31) Chen, X. F.; Chen, X.; Tang, J.; Fei, Z.; Cui, M.; Qiao, X. Macrokinetics for Synthesis of Cyclohexyl Acetate by Esterification of Cyclohexene and Acetic Acid. *Petrochem. Technol.* **2015**, *44*, 833−838.
(32) Hussain, A.; Chaniago, Y. D.; Riaz, A.; Lee, M. Design method for the feasibility and technical evaluation of side-reactor column configurations. *Chem. Eng. Process.* **2019**, *144*, No. 107648.
(33) Chen, X.; Li, Y. P.; Xu, G.; Tang, J. H.; Zhang, Z. X.; Chen, M.; Fei, Z. Y.; Cui, M. F.; Qiao, X. A novel process integrating vacuum distillation with atmospheric chlorination reaction for flexible production of tetrachloroethane and pentachloroethane. *Chin. J. Chem. Eng.* **2018**, *26*, 786−794.
(34) Kaymak, D. B.; Luyben, W. L. Optimum design of a column/side reactor process. *Ind. Eng. Chem. Res.* **2007**, *46*, 5175−5185.
(35) Luyben, W. L.; Yu, C.-C. *Reactive Distillation Design and Control*; John Wiley & Sons, Inc., 2008.
(36) Douglas, J. M. *Conceptual Design of Chemical Process*; McGraw-Hill: New York, 1988.
(37) Geng, X. L.; Zhou, H.; Yan, P.; Li, H.; Li, X. G.; Gao, X. Exergy, economic and environmental analysis of an integrated pressure-swing reactive distillation process for the isobutyl acetate production via methyl acetate transesterification. *Process Saf. Environ. Prot.* **2022**, *158*, 525−536.
(38) Yang, A.; Su, Y.; Teng, L. M.; Jin, S. M.; Zhou, T.; Shen, W. F. Investigation of energy-efficient and sustainable reactive/pressure-swing distillation processes to recover tetrahydrofuran and ethanol from the industrial effluent. *Sep. Purif. Technol.* **2020**, *250*, No. 117210.
(39) Babaie, O.; Esfahany, M. N. Optimization and heat integration of hybrid R-HIDiC and pervaporation by combining GA and PSO algorithm in TAME synthesis. *Sep. Purif. Technol.* **2020**, *236*, No. 116288.
(40) Luyben, W. L. *Distillation Design and Control Using Aspen^{TM} Simulation*; John Wiley & Sons, Inc., 2013.
(41) Luyben, W. L. Control of ternary reactive distillation columns with and without chemically inert components. *Ind. Eng. Chem. Res.* **2007**, *46*, 5576−5590.

https://doi.org/10.1021/acsomega.3c00469
ACS Omega 2023, 8, 13192−13201